

Article

Characterization of a Surface Reaction by means of Atomic Force Microscopy

Florian Albrecht, Niko Pavlišek, Coral Herranz-Lancho, Mario Ruben, and Jascha Repp

J. Am. Chem. Soc., **Just Accepted Manuscript** • DOI: 10.1021/jacs.5b03114 • Publication Date (Web): 24 May 2015

Downloaded from <http://pubs.acs.org> on May 29, 2015

Just Accepted

“Just Accepted” manuscripts have been peer-reviewed and accepted for publication. They are posted online prior to technical editing, formatting for publication and author proofing. The American Chemical Society provides “Just Accepted” as a free service to the research community to expedite the dissemination of scientific material as soon as possible after acceptance. “Just Accepted” manuscripts appear in full in PDF format accompanied by an HTML abstract. “Just Accepted” manuscripts have been fully peer reviewed, but should not be considered the official version of record. They are accessible to all readers and citable by the Digital Object Identifier (DOI®). “Just Accepted” is an optional service offered to authors. Therefore, the “Just Accepted” Web site may not include all articles that will be published in the journal. After a manuscript is technically edited and formatted, it will be removed from the “Just Accepted” Web site and published as an ASAP article. Note that technical editing may introduce minor changes to the manuscript text and/or graphics which could affect content, and all legal disclaimers and ethical guidelines that apply to the journal pertain. ACS cannot be held responsible for errors or consequences arising from the use of information contained in these “Just Accepted” manuscripts.



Characterization of a Surface Reaction by means of Atomic Force Microscopy

Florian Albrecht,^{*,†} Niko Pavliček,^{†,¶} Coral Herranz-Lancho,[‡] Mario Ruben,^{‡,§}
and Jascha Repp[†]

*Institute of Experimental and Applied Physics, University of Regensburg, 93053
Regensburg, Germany, and Institute of Nanotechnology (INT), Karlsruhe Institute of
Technology (KIT), 76344 Eggenstein-Leopoldshafen, Germany*

E-mail: Florian.Albrecht@ur.de

Abstract

We study a thermally-activated on-surface planarization reaction by a detailed analysis of the reactant and reaction products from atomically-resolved atomic force microscopy (AFM) images and spectroscopy. The three-dimensional (3D) structure of the reactant, a helical diphenanthrene derivative, requires going beyond constant-height imaging. The characterization in three dimensions is enabled by acquisition and analysis of the AFM signal in a 3D dataset. This way, the structure and geometry of non-planar molecules as well as their reaction products on terraces and at step edges can be determined.

*To whom correspondence should be addressed

[†]Institute of Experimental and Applied Physics, University of Regensburg, 93053 Regensburg, Germany

[‡]Institute of Nanotechnology (INT), Karlsruhe Institute of Technology (KIT), 76344 Eggenstein-Leopoldshafen, Germany

[¶]Current address: IBM Research–Zurich, 8803 Rüschlikon, Switzerland

[§]Institut de Physique et Chimie des Matériaux de Strasbourg (IMCMS), CNRS-Université de Strasbourg, 67034 Strasbourg, France

Keywords

Atomic Force Microscopy, Single Molecule Chemistry, Surface Chemistry

Introduction

By introducing CO-functionalized tips in frequency-modulated atomic force microscopy (FM-AFM) Gross and coworkers directly resolved the chemical structure of individual planar molecules¹ in real space. Inspired by this novel possibility, the technique has been applied to identify the structure of an unknown molecule,² to resolve the structure of reaction products in single molecule chemistry^{3,4} as well as in thermally-induced on-surface chemical reactions.^{5,6} To avoid additional complexity in these demanding experiments, mostly planar molecules were studied, so that the structure determination could be achieved in the basic imaging mode, in which the tip is scanned in constant height over the sample. For select cases of non-planar structures, the molecule was still flat enough to resolve its geometry.⁷⁻¹⁰ To quantify slight deviations from a flat configuration, as e.g. an overall small tilt of the molecular plane with respect to the surface it is adsorbed on, FM-AFM spectroscopy was employed more recently.¹¹

Most chemical reactions, however, involve three-dimensional (3D) molecular structures. In addition, the reaction pathway is critical for the reaction product. Although many catalytically activated reactions involve the presence of surfaces, on-surface chemistry and its reaction pathways are still poorly understood. In particular, the presence of a surface will strongly affect the possible reaction pathways – at least by restricting the molecular geometry.

Here, we study a thermally-activated on-surface reaction by a detailed analysis of reactant and reaction products from atomically-resolved FM-AFM images and 3D spectroscopy. To analyze the on-surface reaction in three dimensions, we extend the constant-height imaging used so far by analyzing the frequency shift along a non-planar surface of a 3D dataset.

1
2
3
4 This way, the orientation and tilt angle of individual carbon rings in the reactant can be
5 determined. Subsequently, these molecules are submitted to an on-surface planarization
6 reaction that is activated by annealing. The reaction products are also atomically resolved
7 in real space from FM-AFM imaging. The comparison of the structures of reaction products
8 and the 3D reactant suggests that the pathway of the on-surface reaction could involve an
9 out-of-surface rotation of one phenanthrene moiety to enable a planarization of the molecule.
10
11
12
13
14
15
16
17

18 Experimental section

19
20
21 The experiments were carried out with a homebuilt combined STM/AFM, operating in
22 ultra-high vacuum at a temperature of 5 K. The AFM's qPlus tuning fork¹² was operated
23 in the frequency modulation mode.¹³ Sub-Ångstrom oscillation amplitudes were used to
24 maximize the lateral resolution.¹⁴ Bias voltages refer to the sample with respect to the tip.
25
26 The Cu(111) single-crystal sample was cleaned by several sputtering and annealing cycles.
27
28 A small amount of CO was dosed onto the surface for tip functionalization.¹ NaCl islands
29 were grown to facilitate the pick-up of CO molecules to the tip apex from these islands. All
30 AFM data was obtained with a CO-terminated tip apex and away from the NaCl islands.
31
32 Individual molecules were sublimed onto the sample being located in the microscope at a
33 temperature of $T \cong 5$ K. Density functional theory (DFT) calculations¹⁵ of the free monomers
34 were performed to obtain the molecular geometry. To confirm the structural assignment from
35 AFM, matrix-assisted laser desorption and ionization – time of flight (MALDI-TOF) based
36 mass spectrometry, nuclear-magnetic resonance (NMR) spectroscopy, and elemental analysis
37 were performed.¹⁶
38
39
40
41
42
43
44
45
46
47
48
49
50
51

52 Results and discussion

53
54
55 Diphenanthro[9,10-b:9',10'-d]thiophene (DPAT) molecules were synthesized from a solid-
56 state reaction under CO₂ atmosphere between phenanthrene and elemental sulfur.^{16,18} The
57
58
59
60

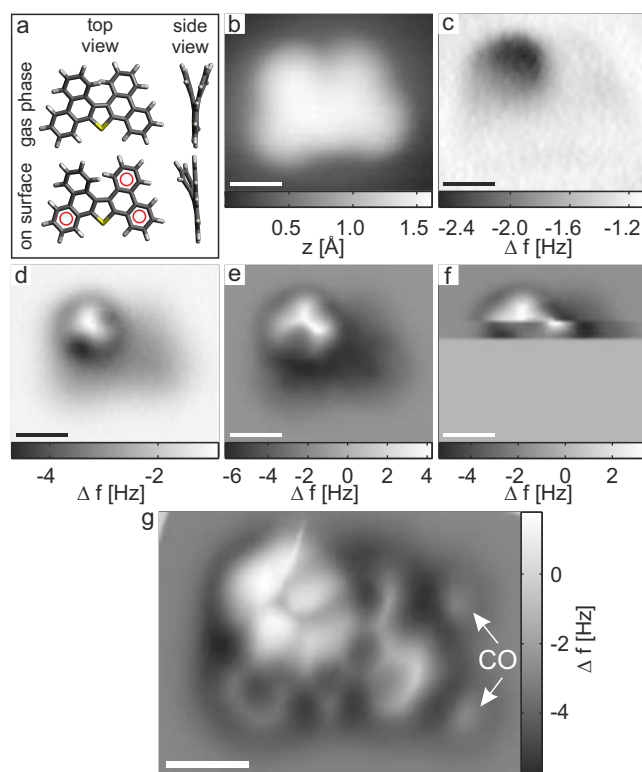


Figure 1: **Characterization of DPAT molecules by means of scanning probe microscopy in standard modes of operation:** **a** Stick models of the molecule's geometry as calculated for the free molecule after full relaxation (top) and with three benzene rings (marked in red) forced to one plane (bottom) to mimic the on-surface geometry, respectively. Carbon, hydrogen and sulfur atoms are represented in black, white and yellow, respectively.¹⁷ **b** and **c** Simultaneously recorded topography (**b**) and frequency shift (**c**) acquired with active current feedback (constant-current mode, $I = 2$ pA, $V = 0.05$ V) **d-f** Set of Δf -images ($\Delta z = 0.3$ Å, 0.5 Å, and 0.7 Å with respect to the STM set point ($I = 2$ pA, $V = 0.1$ V)) of one DPAT molecule on clean copper. **g** Δf -image ($\Delta z = 2.0$ Å with respect to the STM set point ($I = 1$ pA, $V = 0.1$ V)) of a DPAT molecule pinned to two CO molecules. (Scale bars 5 Å)

1
2
3 molecule in the gas phase is non-planar because of steric hindrance. The two phenanthrene
4 moieties are bent out-of-plane at the side opposing the sulfur atom, thus giving rise to a
5 helical shape of the molecule. Its structure as calculated from DFT¹⁵ is displayed in Fig. 1a.
6
7 Provided that DPAT remains intact, adsorption onto the Cu(111) surface will break the
8 symmetry between the two phenanthrene moieties since only one of them can directly face
9 the surface. Interestingly, this asymmetry is not apparent in the topography of a constant
10 current image, as depicted in Fig. 1b. However, the simultaneously recorded frequency
11 shift channel (Fig. 1c) shows a clear asymmetry between the two phenanthrene moieties.¹⁹
12
13 Figures 1d–g show several constant-height AFM images of the molecule at decreasing tip-
14 sample distances. Note that in Fig. 1g the two CO molecules adsorbed next to the DPAT
15 molecule stabilized the molecule against lateral displacement. Similar imaging attempts
16 without CO molecules next to the DPAT molecule resulted in lateral displacement of the
17 molecule in such a way that it could not be stably imaged (Fig. 1f). At the upper left part
18 of Fig. 1d, the repulsive interaction sets in at considerably larger tip height than over the
19 rest of the molecule. Hence, this part of the molecule has to be pointing out towards the tip.
20
21 Otherwise, the image acquired at closest tip-sample distance carries most of the information:
22 four of the benzene rings are readily identified and seem to be oriented roughly parallel to
23 the sample surface – all at a comparable adsorption height. This can be deduced from the
24 intramolecular contrast being relatively homogeneous over these four benzene rings. This
25 suggests that the phenanthrene moiety facing the surface (to the right in Fig. 1g) is flattened
26 out upon adsorption, whereas the other one bends even further due to steric hindrance. There
27 is one atom exhibiting a bond angle slightly smaller than 90°, whereas all other atoms show
28 approximately the 120° bond angles expected for sp²-hybridized carbon atoms. This suggests
29 that the atom with the smaller bond angle is sulfur. Whereas one can guess from the image
30 that the sulfur atom is part of a five-membered ring structure, the part of the molecule that
31 sticks out of the surface plane cannot be identified, and it only leads to the strongly distorted
32 part of the AFM image.
33
34
35
36
37
38
39
40
41
42
43
44
45
46
47
48
49
50
51
52
53
54
55
56
57
58
59
60

1
2
3
4 To also resolve the structure for this part of the molecule, we acquired a three-dimensional
5 (3D) data set of frequency shift Δf as a function of all coordinates x , y and z , by recording
6 $\Delta f(z)$ versus distance z at a closely spaced grid in the surface plane x , y . To avoid too
7 strong tip-sample interaction at close distances z , each of the $\Delta f(z)$ spectra was aborted
8 upon reaching a predefined Δf value as proposed and described by Mohn et al.²⁰ With this
9 dataset, we can extract and display the data for any arbitrary plane within the 3D dataset.
10 The analysis of such 3D imaging is shown in Figure 2. By a variation of the orientation of
11 such planes and looking at the resulting images, one can unambiguously resolve the remaining
12 structure of the molecule. Furthermore, as the orientations of the imaging planes are set,
13 this technique allows us to extract the out-of-plane distortion angles of the molecule within
14 to a few degrees uncertainty. Based on this analysis, we can identify the molecular structure
15 itself as well as its 3D geometry after adsorption, despite the out-of-plane rotation of one of
16 the benzene rings being as large as $\simeq 23^\circ$. This possibility to resolve the 3D geometry of
17 molecules is not at all self-evident, because at some even larger tilt angle one may expect
18 that the CO bending at the tip apex²¹ prevents a structural analysis.
19
20
21
22
23
24
25
26
27
28
29
30
31
32
33

34 To verify our structural assignment, we performed MALDI-TOF and NMR¹⁶ measure-
35 ments of the molecules. Both mass and NMR spectra fully support our structural analysis.
36 Note that, without expecting the reaction product that was identified from AFM, the NMR
37 spectrum is not easily converted into a structural model. To further analyze the geometry
38 of the molecule, we mimicked the flattening of one phenanthrene moiety upon adsorption in
39 the geometry calculations by forcing three of the carbon rings to be planar, and by letting
40 the rest of the molecule relax. The resulting geometry fits very well to the geometry deduced
41 from AFM data, as can be seen in Fig. 2, including the out-of-surface tilt angles of $\simeq 10^\circ$
42 and $\simeq 23^\circ$, respectively.
43
44
45
46
47
48
49
50
51

52 The molecular structure and the strong out-of-plane distortion suggest that the molecule
53 can be planarized by annealing. In analogy to other on-surface-reactions^{22,23} one might
54 expect a ring closure by a C–C bond formation at the position of steric hindrance resulting
55
56
57
58
59
60

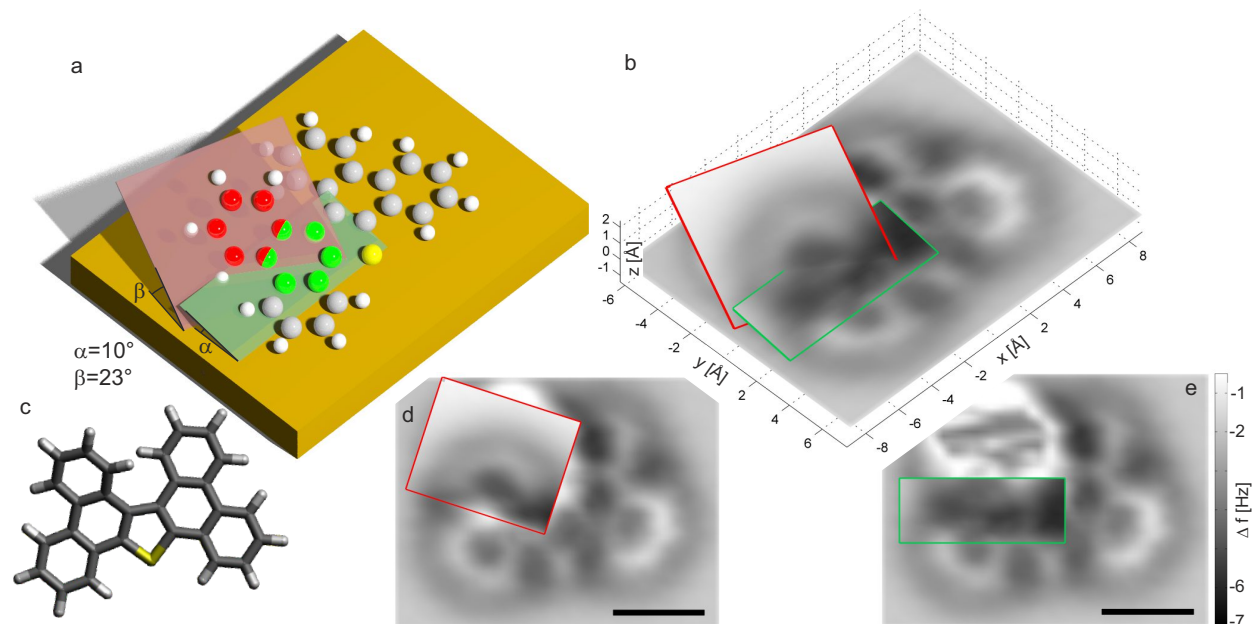


Figure 2: **Molecular structure identification from 3D dataset:** To resolve the molecular structure from Δf imaging, the 3D dataset is displayed along three different planar cross sections. While one of them is parallel to the surface, the other two are aligned with respect to the two carbon rings that are tilted with respect to the surface (green and red). **a** 3D representation of molecular structure including the cross-sections, along which the experimental data is displayed in **b**. **c** Top view of the geometric structure for reference.¹⁷ **d** and **e** Top views of 3D data with only one of the tilted cross sections in each panel (scale bars 5 Å).

in a C_{2v} -symmetric molecule¹⁸ (having C_S -symmetry when adsorbed).

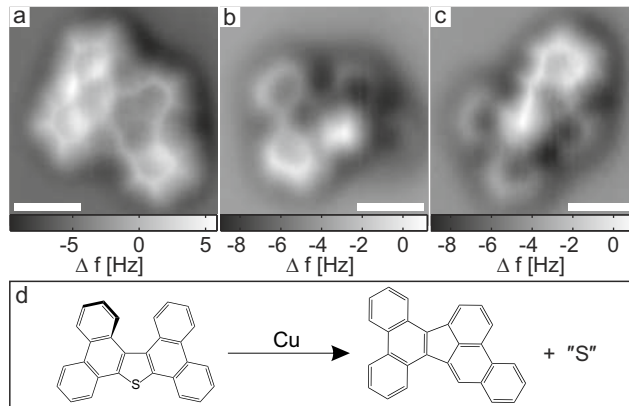


Figure 3: **Reaction products:** **a-c** Constant height Δf -images of different reaction products. All products are planar (**a**) or almost planar (**b** and **c**), so that the two phenanthrene moieties can be clearly identified. The latter are attached to each other in a non-symmetric way and are clearly *not* aligned (anti-) parallel. Imaging parameters: $\Delta z = 3.2 \text{ \AA}$, $\Delta z = 2.55 \text{ \AA}$, and $\Delta z = 2.75 \text{ \AA}$ with respect to the STM set point ($I = 1 \text{ pA}$, $V = 0.1 \text{ V}$) (Scale bars 5 \AA) **d** Reaction scheme for planar product.

To activate such an on-surface-reaction, we annealed the sample to $200 \text{ }^\circ\text{C}$. After annealing, we analyzed 32 individual molecules from atomically resolved AFM images. Further molecules were identified to be of the same species as some of the atomically resolved ones from their appearance in scanning tunneling microscopy images (not shown). Via the atomically resolved AFM images we found four different species, which together account for 30 out of the 32 individual molecules. The remaining two individual molecules must have formed from more than just a single reactant and are disregarded here. One of the four species is the non-reacted DPAT molecule. This observation confirms that the anneal temperature is just at the verge of initiating the reaction. From the annealing time of two minutes and the observation that 25 out of 30 molecules have reacted, we estimate an activation energy of $\approx 1.4 \text{ eV}$. The constant-height AFM images of the three remaining species are shown in Fig. 3a–c. One of the latter is completely planar, so that its structure can be readily identified from the AFM image (see Fig. 3a and d) as phenanthro(9,10-*e*)acephenanthrylene.²⁴ None of the bond angles is particularly small, which may indicate that the sulfur was eliminated from the molecule. The molecule does *not* have an out-of-plane mirror symmetry that would

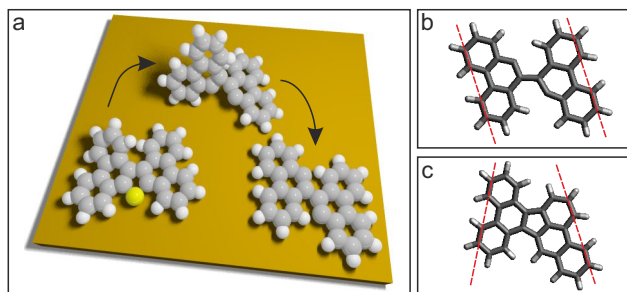


Figure 4: **A potential reaction pathway:** **a** 3D representation of the proposed reaction pathway starting with DPAT on the left hand side. The experimentally observed non-symmetric arrangement of the two phenanthrene moieties can be explained by a reaction pathway involving an out-of-plane rotation of one of the phenanthrene moieties as depicted by the models from left to right. **b** and **c** stick models of planar reaction products without (**b**) and with (**c**) pentagonal ring closure, respectively. The dashed red lines highlight the different alignment of the phenanthrene moieties in both cases. In comparison, all the experimentally observed structures indicate a ring closure in their center. Molecular models in panels **b** and **c** were structurally optimized and displayed using Avogadro.¹⁷

be expected for the simple reaction pathway for planarization discussed above.¹⁸ Instead, the two phenanthrene moieties are now connected to each other at the center of the molecule with different orientations.

Apart from the planar reaction product shown in Fig. 3a, there are two more species, displayed in Fig. 3b and c, that are not completely planar. While the entire structure is not directly apparent from their AFM images, these do allow for an identification of the orientation of the two phenanthrene moieties. In both cases, the orientation agrees with the one of the planar reaction product. As the central part of the molecule cannot be imaged so clearly, it is at first glance unclear whether a five-membered ring has formed at their center in analogy to the planar reaction product. However, the five-membered ring enforces an orientation of the two phenanthrene moieties in an angle of 150° , whereas a single bond between the two would result in an angle of 180° (see Fig. 4b and c). As the observed angle in the AFM images agrees with the former, we conclude that the five-membered ring has to be present. Most probably, the sulfur atom is still present in these molecular structures, giving rise to the additional feature at the center of the target molecule.

Hence, from the AFM images one can assign the backbone of all three products as

1
2
3 phenanthro(9,10-*e*)acephenanthrylene – a molecule that has been synthesized from phenan-
4 threne, using wet chemistry.²⁵
5
6

7 We now turn to the discussion of a potential pathway of the observed reaction. By
8 comparing the reactant and the product (see Fig. 3d) and their respective symmetries one
9 realizes that the two phenantrene moieties are interconnected quite differently. As illustrated
10 in Fig. 4a, a reaction pathway involving the sulfur atom elimination, an (almost) 180° out-
11 of-plane rotation of one of them, and, finally, a ring closure yield the observed molecular
12 structure. Note that, after a bond cleavage at the sulfur atom, the two phenantrene moieties
13 are connected by a single σ -bond only, facilitating the rotation. Without such an out-of-
14 plane rotation, a reorganization of *both* bonds that connect the two phenantrene moieties
15 would be required. Such a pathway would not be easily reconciled with the observation of
16 almost all reaction products still consisting of two phenantrenes – though we cannot exclude
17 such bond reorganization from our data. We therefore propose C–S bond cleavage, the out-
18 of-plane rotation of one phenantrene moiety, and a ring closure as the reaction pathway. As
19 has been observed previously,^{26,27} the surface can coordinate atoms with open bonds that
20 occur from e. g. the sulfur elimination and thereby stabilize intermediate structures, such
21 as the one displayed in Fig. 4b. It may well be that the hydrogen that is released upon
22 pentagonal ring closure will saturate the open bond in the final product as shown in Fig. 4c.
23 While the planar structure of the reaction product may indicate the saturation of all bonds
24 by hydrogen atoms, we cannot exclude that instead the respective atoms are coordinated to
25 the substrate.
26
27
28
29
30
31
32
33
34
35
36
37
38
39
40
41
42
43
44
45

46 In contrast to our observation, in an earlier work¹⁸ the symmetric reaction product
47 dibenzo[2,3:10,11]perlylo[1,12-*bcd*]thiophene was obtained from DPAT molecules in the pres-
48 ence of copper particles serving as a catalytic surface. It is well known that at step edges
49 the reactivity of the substrate is enhanced^{26,28,29} which possibly enables alternative reaction
50 pathways. Bearing this in mind, we imaged substrate defect step edges, to which molecules
51 are attached, after annealing. Interestingly, in a corresponding AFM image displayed in
52
53
54
55
56
57
58
59
60

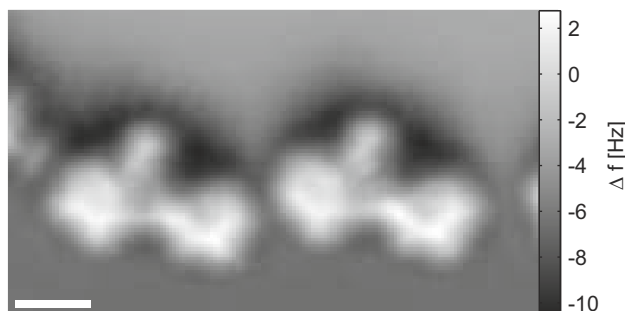


Figure 5: **Reaction products at substrate step edge:** AFM image of phenanthrene units attached to a copper step edge after sample annealing. The higher reactivity at step edges apparently facilitates dissociation of molecules. Imaging parameters: $\Delta z = 1.55 \text{ \AA}$ with respect to the STM set point ($I = 1 \text{ pA}$, $V = 0.1 \text{ V}$) at the lower laying terrace in the top part of the image. (Scale bar 5 \AA)

Fig. 5 we find planar molecules that can be readily identified as containing one of the two phenanthrene moieties only. Hence, step edges obviously facilitate the dissociation of the molecules separating the two phenanthrene moieties. This observation resolves the apparent contradiction of different reactions, as one might speculate that at even higher anneal temperatures the two phenanthrenes can reunite to form a symmetric reaction product.

Conclusion

In summary, we analyzed the non-planar adsorption geometry of DPAT molecules adsorbed on Cu(111) from atomically resolved 3D FM-AFM data. Upon annealing, the molecules undergo an on-surface planarization reaction. The reaction pathway is proposed to involve (i) C–S bond cleavage (ii) an (almost) 180° out-of-plane rotation of one phenanthrene moiety, and (iii) aromatization by dehydrogenation. Finally, the higher reactivity at step edges leads to a dissociation of the molecule separating the two phenanthrene moieties.

Acknowledgement

The authors would like to thank Andreas Pöllmann for support. Financial support from the Deutsche Forschungsgemeinschaft (GRK 1570, RE 2669/4-1, SPP 1243 and SPP 1459),

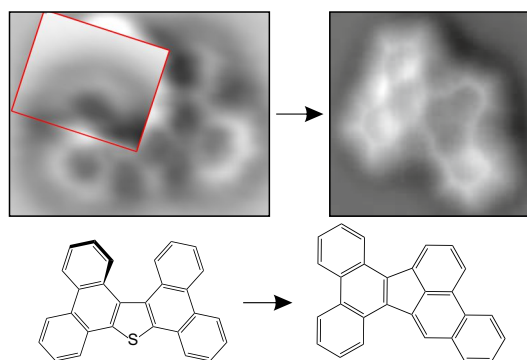
1
2
3 the Volkswagen Foundation through its Lichtenberg program and the Marie-Curie ITN
4
5 “SMALL” (grant agreement: 238804) is gratefully acknowledged.
6
7

8 9 10 **References**

- 11
12 (1) Gross, L.; Mohn, F.; Moll, N.; Liljeroth, P.; Meyer, G. *Science* **2009**, *325*, 1110.
13
14
15 (2) Gross, L.; Mohn, F.; Moll, N.; Meyer, G.; Ebel, R.; Abdel-Mageed, W. M.; Jaspars, M.
16
17 *Nature Chem.* **2010**, *2*, 821.
18
19
20 (3) Mohn, F.; Repp, J.; Gross, L.; Meyer, G.; Dyer, M. S.; Persson, M. *Phys. Rev. Lett.*
21
22 **2010**, *105*, 266102.
23
24
25 (4) Albrecht, F.; Neu, M.; Quest, C.; Swart, I.; Repp, J. *J. Am. Chem. Soc.* **2013**, *135*,
26
27 9200.
28
29
30 (5) de Oteyza, D. G.; Gorman, P.; Chen, Y.-C.; Wickenburg, S.; Riss, A.; Mowbray, D. J.;
31
32 Etkin, G.; Pedramrazi, Z.; Tsai, H.-Z.; Rubio, A.; Crommie, M. F.; Fischer, F. R.
33
34 *Science* **2013**, *340*, 1434.
35
36
37 (6) Riss, A.; Wickenburg, S.; Gorman, P.; Tan, L. Z.; Tsai, H.-Z.; de Oteyza, D. G.;
38
39 Chen, Y.-C.; Bradley, A. J.; Ugeda, M. M.; Etkin, G.; Louie, S. G.; Fischer, F. R.;
40
41 Crommie, M. F. *Nano Lett.* **2014**, *14*, 2251.
42
43
44 (7) Pavliček, N.; Fleury, B.; Neu, M.; Niedenführ, J.; Herranz-Lancho, C.; Ruben, M.;
45
46 Repp, J. *Phys. Rev. Lett.* **2012**, *108*, 086101.
47
48
49 (8) Hanssen, K. .; Schuler, B.; Williams, A. J.; Demissie, T. B.; Hansen, E.; Andersen, J. H.;
50
51 Svenson, J.; Blinov, K.; Repisky, M.; Mohn, F.; Meyer, G.; Svendsen, J.-S.; Ruud, K.;
52
53 Elyashberg, M.; Gross, L.; Jaspars, M.; Isaksson, J., *Angew. Chem. Int. Ed.* **2012**, *51*,
54
55 12238.
56
57
58
59
60

- 1
2
3
4 (9) Pavliček, N.; Herranz-Lancho, C.; Fleury, B.; Neu, M.; Niedenführ, J.; Ruben, M.;
5 Repp, J. *physica status solidi (b)* **2013**, *250*, 2424.
6
7
8
9 (10) Schuler, B.; Liu, S.-X.; Geng, Y.; Decurtins, S.; Meyer, G.; Gross, L. *Nano Lett.* **2014**,
10 *14*, 3342.
11
12
13 (11) Schuler, B.; Liu, W.; Tkatchenko, A.; Moll, N.; Meyer, G.; Mistry, A.; Fox, D.; Gross, L.
14 *Phys. Rev. Lett.* **2013**, *111*, 106103.
15
16
17
18 (12) Giessibl, F. *J. Appl. Phys. Lett.* **2000**, *76*, 1470.
19
20
21 (13) Albrecht, T. R.; Grütter, P.; Horne, D.; Rugar, D. *J. Appl. Phys.* **1991**, *69*, 668.
22
23
24 (14) Giessibl, F. *J. Rev. Mod. Phys.* **2003**, *75*, 949.
25
26
27 (15) CPMD V3.15 Copyright IBM Corp 1990-2011, Copyright MPI fuer Festkoerper-
28 forschung Stuttgart 1997-2001.
29
30
31
32 (16) Herranz-Lancho, C. Synthesis and Characterization of Molecules for Electronic Devices.
33 Ph.D. thesis, Université de Strasbourg, 2013.
34
35
36
37 (17) Molecular models are displayed using Avogadro – an open-source molecular builder and
38 visualization tool. Version 1.1.0 <http://avogadro.openmolecules.net/>.
39
40
41
42 (18) Zander, M.; Franke, W. H. *Chem. Ber.* **1973**, *106*, 2752.
43
44
45 (19) In constant current imaging mode, the Δf -signal is influenced by the z-feedback. How-
46 ever, the Δf -image shows much more asymmetry between the two phenanthrene units
47 than the topography.
48
49
50
51 (20) Mohn, F.; Gross, L.; Meyer, G. *Appl. Phys. Lett.* **2011**, *99*, 53106.
52
53
54 (21) Moll, N.; Gross, L.; Mohn, F.; Curioni, A.; Meyer, G. *New J. Phys.* **2010**, *12*, 125020.
55
56
57
58
59
60

- 1
2
3
4
5
6
7
8
9
10
11
12
13
14
15
16
17
18
19
20
21
22
23
24
25
26
27
28
29
30
31
32
33
34
35
- (22) Cai, J.; Ruffieux, P.; Jaafar, R.; Bieri, M.; Braun, T.; Blankenburg, S.; Muoth, M.; Seitsonen, A. P.; Saleh, M.; Feng, X.; Müllen, K.; Fasel, R. *Nature* **2010**, *466*, 470.
- (23) Treier, M.; Pignedoli, C. A.; Laino, T.; Rieger, R.; Müllen, K.; Passerone, D.; Fasel, R. *Nature Chem.* **2011**, *3*, 61.
- (24) We cannot exclude partial dehydrogenation of the reaction product on the surface.
- (25) Franck, H.-G.; Buffleb, H. *Liebigs Ann. Chem.* **1967**, *701*, 53.
- (26) Hla, S.-W.; Bartels, L.; Meyer, G.; Rieder, K.-H. *Phys. Rev. Lett.* **2000**, *85*, 2777.
- (27) Zhao, A.; Li, Q.; Chen, L.; Xiang, H.; Wang, W.; Pan, S.; Wang, B.; Xiao, X.; Yang, J.; Hou, J. G.; Zhu, Q. *Science* **2005**, *309*, 1542.
- (28) Dahl, S.; Logadottir, A.; Egeberg, R. C.; Larsen, J. H.; Chorkendorff, I.; Törnqvist, E.; Nørskov, J. K. *Phys. Rev. Lett.* **1999**, *83*, 1814.
- (29) Vang, R. T.; Honkala, K.; Dahl, S.; Vestergaard, E. K.; Schnadt, J.; Lægsgaard, E.; Clausen, B. S.; Nørskov, J. K.; Besenbacher, F. *Nature Mater.* **2005**, *4*, 160.



49
50
51
52
53
54
55
56
57
58
59
60

Figure 6: TOC figure